Experimental Study on a Rectangular Variable Intake for Space Planes

T. Kojima[*], *H. Taguchi*[†], *K. Okai*[*], *H. Futamura*[‡]
JAXA (Japan Aerospace Exploration Agency, the Institute of Space Technology and Aeronautics),
7-44-1 Jindaijihigashi-machi, Chofu Tokyo 182-8522 Japan
E-mail: kojma.takayuki@jaxa.jp

and

Y. Maru[§]
University of Tokyo, Tokyo, Japan

Keywords: Intake, Wind tunnel test, Air breathing engine

Abstract

Hypersonic wind tunnel test of the rectangular variable geometry intake is performed. For realization of a Precooled turbojet engine, development of a hypersonic ramjet engine is planned. To investigate performance of the intake of the hypersonic ramjet engine, wind tunnel test is done with freestream Mach number of 5.1. The total pressure recovery was 18 % with 12.9 % of ramp bleed. Several reasons for low total pressure recovery are shown. Supersonic internal compression is not enough. Then, the throat Mach number is high (M2.61) and total pressure losses at the terminal shock is large. Supersonic flow at the throat and position of the terminal shock is sensitive to a difference of the second ramp 's throat height and the third ramp 's throat height. Flow separations at the second ramp 's trailing edge and the third ramp 's leading edge are seen those could result in the trigger of unstart. The seal mechanism between the ramps and the sidewalls is important.

Introduction

Many concepts of TBCC engines are proposed recently in Japan [1, 2]. Figure 1 shows a Precooled turbojet engine that is to be operative between sea-level and Mach 6. Hypersonic aerodynamic components such as an air intake and variable nozzle are key components to materialize those advanced propulsion systems. Then wind tunnel tests and flight tests of a small scale hypersonic ramjet engine model (Figure 2) are planned so that the effective operation of the intake and the nozzle would be proved.

A study of the hypersonic air intake was started in 1999. After parametric design studies on rectangular type intakes, configuration of the intake was designed. The design was carried out two-dimensionally assuming a flow was completely two dimensional. Furthermore, the configuration was designed to optimize the flow at Mach 6. A hypersonic wind tunnel test was carried out to acquire off-design performance and ideas to improve these performances, besides a two-dimensional CFD analysis [3].

* Aeroengine Testing Technology Center
†Future Space Transportation Research Center
‡Aeronautical Environment Technology Center
§Department of Aeronautics and Astronautics, Doctor course

Test model design and performance estimation

Design

The conceptual drawing of the rectangular intake is shown in Figure 3. For the simplicity of the variable system, two oblique shocks are used as an external compression. Number of oblique shocks inside the cowl varies from 2 to 7 depending on freestream Mach number. Variable system is limited to the second ramps and the third ramps. For the reduction in the driving force of the ramps, air flow is bifurcated. Pressure inside of the second ramps is higher than the pressure outside of the second ramps and pressure inside the third ramps is lower than the pressure outside of the third ramps. Then the ramp driving forces for the second ramps and third ramps are canceled each other [4].

Performance estimation by one-dimensional analysis and CFD

Intake aerodynamic performances were estimated by both two-dimensional analysis and CFD. The scale of the intake is 450 mm in cowl height that will be applied for the Precooled turbojet engine (Figure 1). For prediction of the design total pressure recovery, total pressure losses caused by the viscosity such as friction loss, separation loss, shock-boundary-layer interaction loss and subsonic diffuser turning loss were taken into account. For the large scaled intake model (cowl height is 450mm) total pressure recovery was 42.9 % including the loss generated by the viscosity at Mach 6 design point.

The configuration of the sidewall can vary

sideway spillage and starting performance of the intake. If the sidewall is extended, the spillage flow to the sideway can be reduced so that that the mass capture of the intake can be improved. However, the extension of the sidewall can reduce the intake starting contraction ratio. A leading edge of the test model was designed to be 60 deg from second ramp leading edge.

Two-dimensional CFD was also conducted so that problems of the design could be revealed. The commercial CFD program GASP is utilized to the CFD [5]. Two-dimensional RANS code was selected as the governing equation for both inviscid and viscous calculation. For viscous calculation, Wilcox k-ω model is used as the turbulence model for all grids. The number of grids is approximately 40000 as shown in Figure 4. The second throat height is adjusted so that the back pressure of the subsonic diffuser is controlled. Reynolds numbers of the calculation were set to match the condition that the small scale ramjet engine (Figure.2, cowl height = 75mm) flies under constant dynamic pressure of 30 kPa for each Mach number.

The result of the Two-dimensional estimation and CFD are summarized in Figure 5. The total pressure recovery of the CFD estimation is low at high Mach number. The throat Mach number is kept about 1.6~1.9 because the intake is unstarted with narrower throat height. Then the loss caused by the terminal shock is larger The terminal shock position is very sensitive to the difference of the second ramp's throat height and the third ramp's throat height. If the third ramp's throat height is smaller, bow shock is generated in front of the leading edge of the third ramp, that could cause unstart.

Fabrication of the wind tunnel test model

The test model is shown in Figure 6 and 7. Intake cross section size is 100mm (width) and 75mm (height) at the cowl inlet. This test model simulates the half of the hypersonic ramjet engine. The variable second ramp and third ramp are connected to the ramp actuator by the links of each ramp. By changing length of the third ramp's link length, the difference of the second ramp's throat height and the third ramp's throat height is changed. Three types of third ramp's link are used during the test (Middle, Long (= Middle +2mm), Short (= Middle -2mm)). As shown in Figure 8, third ramp's throat height of the long link is always narrower for all actuator position. A boundary layer on the ramp is removed through the ramp cavity. The ramp bleed flow rate is changed by the orifice installed at the bleed flow exit. Three bleed flow control orifices are used at the test (0mm, 20mm, 40mm). Boundary layer on the cowl is removed from porous cowl bleed holes. 143 holes are drilled normally to the cowl at the throat. A diameter of the holes is 1 mm. A back pressure of the intake is controlled by moving the exit valve up and down.

Test Condition

Wind tunnel conditions are set as follows: Mach number = 5.1 ± 0.07, Total Pressure = 1.0 ± 0.005 MPa, Total Temperature = 650 ± 25 K, Test Duration = 60 sec. Reynolds numbers are compared in Table 1 between the wind tunnel test condition and the engine's flight condition. Reynolds number of the wind tunnel test is about twice of the hypersonic ramjet flight condition. A distance of a transition of the boundary layer is estimated between 300 mm and 700 mm

Intake performances are acquired by following sequences.

(a) Move ramp from full open to full close to investigate a unstart ramp position. Exit valve is kept full open.

(b) Ramp is fixed to the position where second ramp's throat height is 110 % of the unstart ramp position that is acquired at the test (a). The exit valve moves from full open to full close. The total pressure recovery of the intake become the largest before unstart.

Total pressure recovery and mass capture ratio are two important parameters of the intake performance. The total pressure recovery is measured using 30 pitot tubes installed at the exit of the intake (750 mm from the ramp leading edge). Area averaged total pressure recovery is used for the performance evaluation. For most of all tests, the area averaged total pressure recovery and flow rate averaged total pressure recovery are almost the same.

Mass capture ratio is estimated from the exit valve throat area and area averaged total pressure recovery assuming that the flow is choked and flow coefficient is unity. Bleed flow rates of the ramp and the cowl are estimated using the cowl static pressure and plenum chamber pressure assuming the flow is chocked and flow coefficient is unity.

Test Result

Intake Performance

Intake performances are summarized in Figure 9. Following results are discussed, from these tests.

(a) The total pressure recovery could achieve 18% with ramp bleed orifice of 40 mm. The bleed flow rate of this condition is 12.9 %. By increasing the ramp bleed flow rate, the total pressure recovery can be increased.

(b) The cowl bleed can increase the total pressure recovery. But the improvement is small.

(c) If the third ramp's throat height is narrower than the second ramp's throat height, the total pressure

recovery drops.
(d) By reducing the second ramp's throat height, the total pressure recovery can be improved.

Total pressure recovery at the intake exit measured by the pitot tubes are visualized in Figure 10. For each picture, diameters of bleed holes of both ramp and cowl are changed. Numbers in parenthesis show the bleed flow rate fractions of the ramp and cowl. Distribution of the total pressure at the center of sidewalls is shown in Figure 11. Following results are discussed:
(a) Without bleed, center of the total pressure recovery distribution is on the cowl side. At the center of the total pressure recovery distribution, the peak total pressure recovery is very high (21 %). However, large total pressure distortion.
(b) By increasing the ramp bleed flow rate, the distortion reduces and the averaged total pressure recovery increases.
(c) If the ramp bleed is increased to 12.9 %, the peak point of the total pressure recovery moves close to the sidewall. Then the ramp bleed can improve the total pressure recovery and three dimensional flow patterns.

Static Pressure distribution is shown in Figure 12. Static pressures of the ramp and cowl are measured at the center between sidewalls. Compression at the exit of the third ramp is not smooth. Interaction of the ramp, the cowl and the sidewalls are expected at the exit of the third ramp.

Comparison between the estimation and the test result

Table 2 shows the Mach number and local total pressure recovery estimated at the test condition. The turning angle of each shocks are estimated from the ramp angle so that the change of the turning angle by the generation of the boundary layer is not included. Because the second ramp's throat height is larger than the design height, numbers of the oblique shocks are limited. As seen from the schlieren picture (Figure 13 (b)), 2 oblique shocks are used as the internal compression. Then, the throat Mach number is expected to be very large (M2.61). Total pressure losses at the subsonic diffuser are shown in Table 3. If the throat Mach number is 2.61, the total pressure downstream of the terminal shock becomes 36.8 %. In this condition, the loss generated the terminal shock is dominant.

Comparison of the mass flow between test result and the estimation is shown in Table 4. Estimated flow ratio through the cowl inlet is 0.914, while test result is 0.772. The angle of the oblique shock form the first and the second ramp is very narrow (14.8 deg and 17.1 deg). Then the change of the shock angle caused by development of the boundary layer effects on the change of the spillage flow rate.

Flow Visualization

Schlieren picture is shown in Figure 13. If the boundary layer is not removed from the ramp, large flow separation (lambda shock) caused by an interaction between the oblique shock from the cowl lip and ramp's boundary layer is seen as shown in (a). This separation can be reduced by the ramp bleeding as seen in (b). However, a separation caused by the terminal shock is still observed (c). After the terminal shock, flow at the ramp side is strongly separated. Then subsonic diffuse of the flow to the cowl side is not effective. When the intake is unstarted (d), strong shock is generated in front of the cowl and small amount of shock oscillation is observed. Intake buzz did not occur.

Oilflow test is carried out to see the three dimensional flow in the intake. Oilflow patterns from cowl side taken during blow of the wind tunnel (a) and from sidewall side taken after the blow (b) are shown in Figure 14. Three dimensional flow is observed from the oilflow pattern. From this oilflow pattern, following informations about an improvement of the intake flow are seen.
(a) Flow separation at the second ramp and the third ramp is seen. The separation at the third ramp occurs where the second ramp separation does not occur. It seems to be necessary to smooth the angle of the second ramp's trailing edge and the third ramp's leading edge.
(b) Flow through the sidewall clearance is seen. The seal mechanism between the sidewalls and the ramps are important.

Concluding Remarks

To investigate the aerodynamic performances of the rectangular intake, wind tunnel test was conducted. Following results were acquired.
- The total pressure recovery was lower than the design. Because the Mach number at the throat could not be reduced, the loss at the terminal shock was large.
- By bleeding the boundary layer on the ramp, the total pressure recovery was increased and the distortion at the intake exit was reduced.
- Flow inside the intake was visualized by an oilflow test. Flow separation at the trailing edge of the second ramp and at the leading edge of the third ramp was found. Flow through the clearance between sidewalls and ramps were seen.

Acknowledgments

The authors gratefully acknowledge the contribution of Dr. Murakami (JAXA) and Dr. Watanabe, Mr. Hirabayashi and all members of the hypersonic wind tunnel for the design, for the wind tunnel test, analysis of the data, and for their support.

References

1. Taguchi, H., "Design Study on Hypersonic Engine Components for TBCC Space Planes," 12th AIAA International Space Planes and Hypersonic Systems and Technologies, AIAA-2003-7006, Norfolk VA, Dec 2003.
2. Sato, T., "Development Study of the ATREX Engine," IAC-03-S.5.02, 54th International Astronautical Congress, Bremen, Oct 2003.
3. Okai, K., "Numerical Analysis of Variable Intake and Nozzle for Hypersonic Engines," 12th AIAA International Space Planes and Hypersonic Systems and Technologies, AIAA-2003-7069, Norfolk VA, Dec 2003.
4. Taguchi, H., "Engines for Hypersonic Airplanes," Japanese Patent 2003-107016, 2003.
5. *Aerosoft GASPex Users Manual, March 1997.*
6. Mattingly, Jack D., "Aircraft Engine Design," AIAA Educational Series, 1988.
7. Sdon, J., ""Intake Aerodynamics," AIAA Educational Series, Washington, 1989.

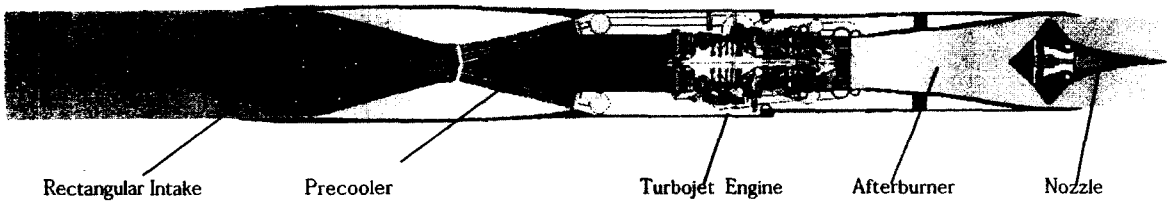

Fig. 1 Precooled turbojet engine

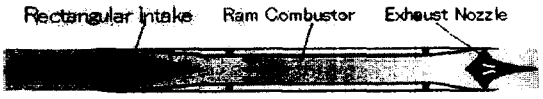

Fig. 2 Hypersonic ramjet engine

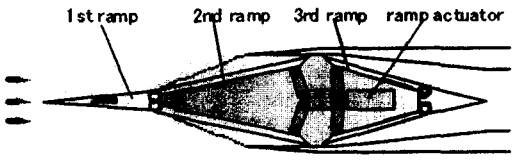

Fig. 3 Variable geometry rectangular intake

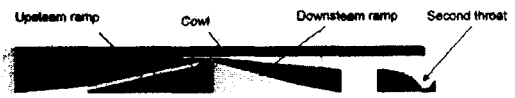

Fig. 4 CFD grid

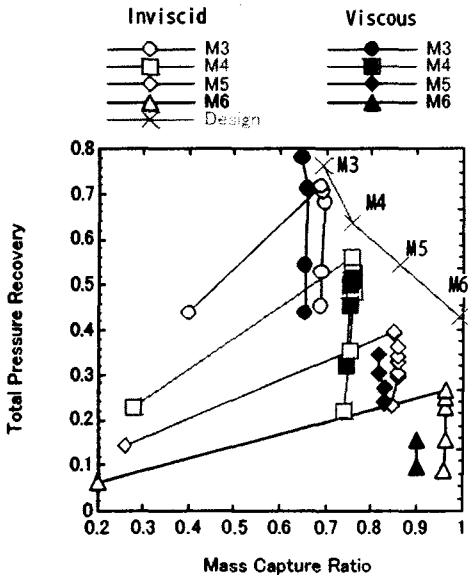

Fig. 5 Rectangular intake aerodynamic performances

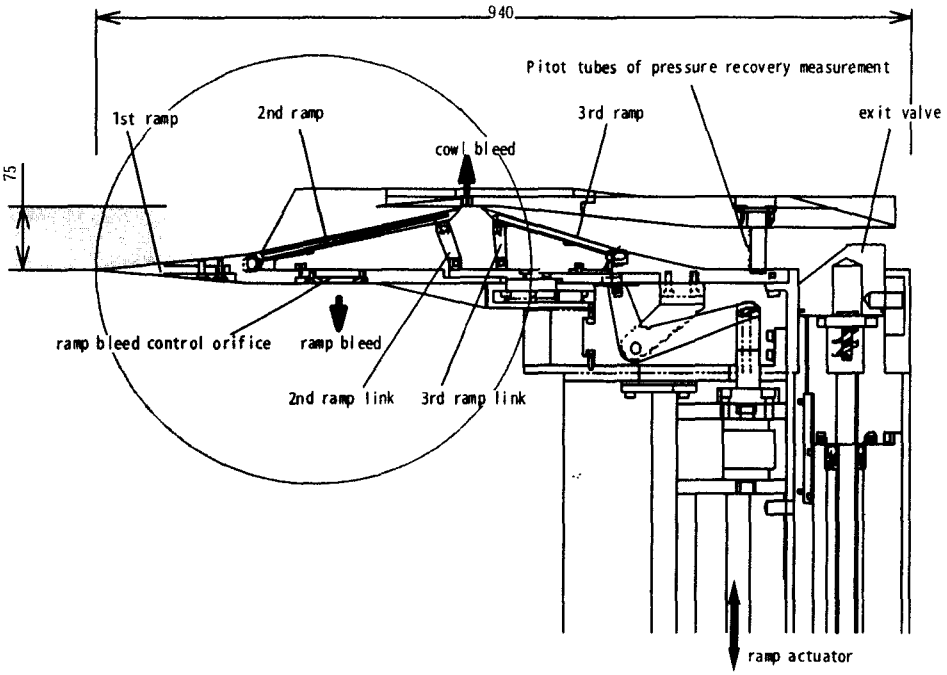

Fig. 6 Wind tunnel test model

Fig. 7 Picture of the Test Model

Table. 1 Reynolds number of the test condition

		Wind Tunnel Test	Precooled Tubojet (Fig. 1)	Hypersonic Ramjet (Fig. 2)
Dynamic Pressure	kPa		50	50
Mach		5.1	5.1	5.1
Total Pressure	MPa	1	1.5	1.5
Total Temperature	K	650	1332	1332
Re/m	/m	8.06E+06	4.35E+06	4.35E+06
Cowl Height	m	0.075	0.45	0.075
Re		6.04E+05	1.96E+06	3.26E+05

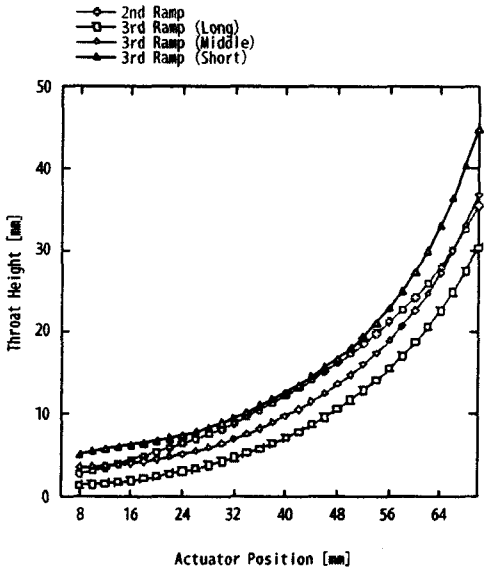

Fig, 8 Throat Height

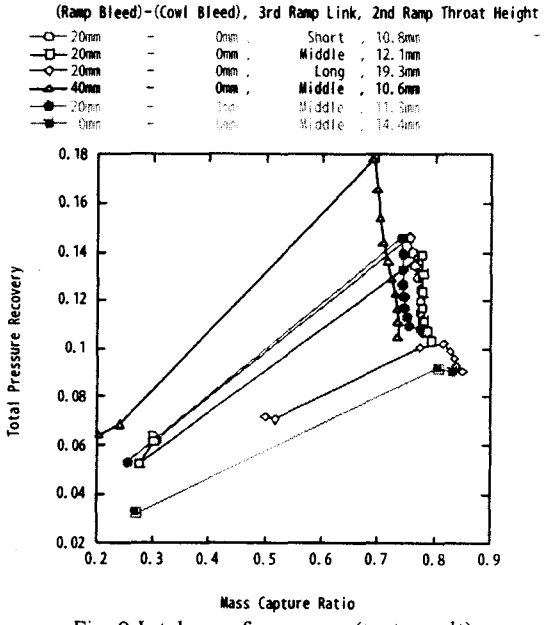

Fig. 9 Intake performances (test result)

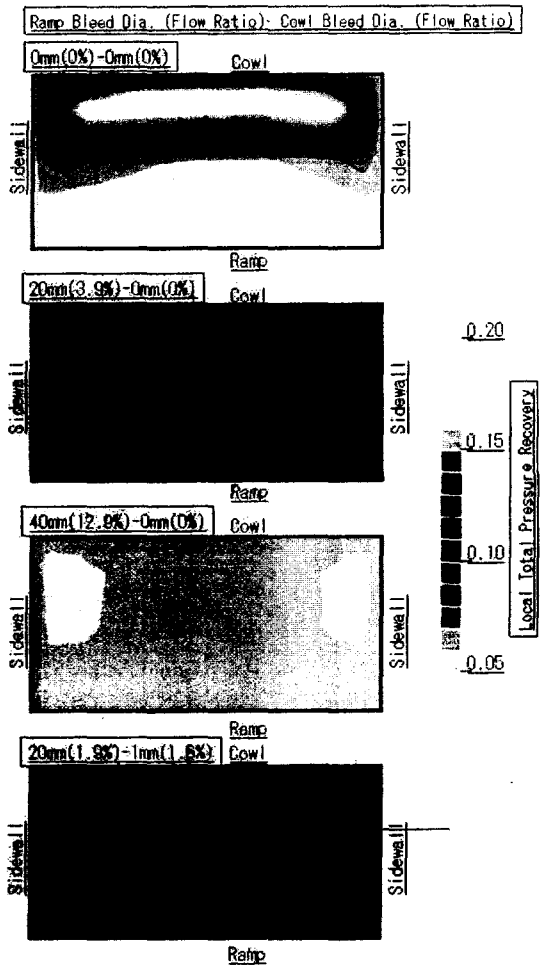

Fig. 10 Total pressure recovery distribution at intake exit (3rd ramp link = Middle)

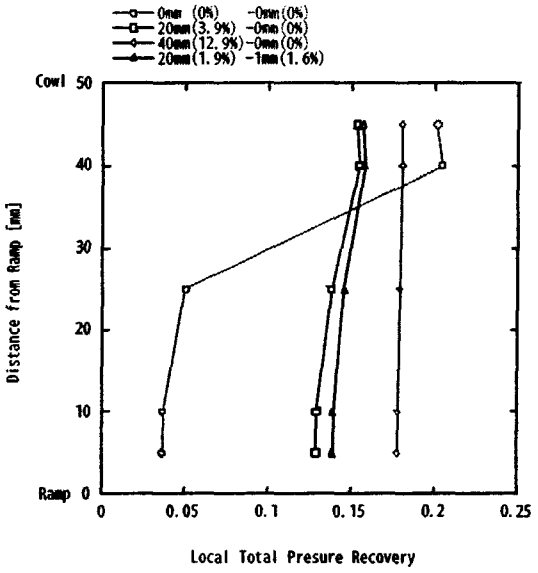

Fig. 11 Total pressure recovery distribution at intake (at center of sidewalls, 3rd ramp link = Middle)

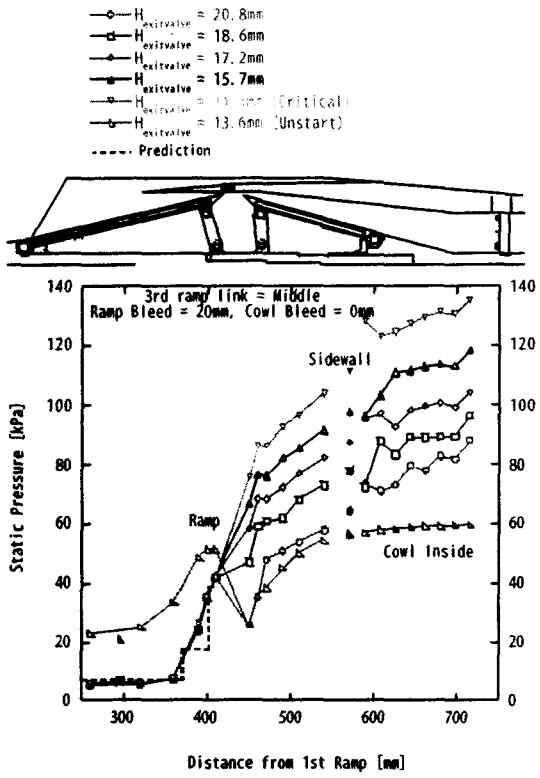

Fig. 12 Static pressure distribution

Table. 2 Total pressure loss estimation (supersonic diffuser)

		Turning Angle (deg)	Mach	Pressure Recovery
	FreeStream		5.1	1
External	1st ramp	5	4.58	0.987
	2nd ramp	6.27	4.03	0.957
Internal	cowl 1st	11.27	3.22	0.859
	ramp 1st	11.27	2.61	0.808
	cowl 2nd	11.27	2.13	0.778

(Ramp Bleed = 20mm, Cowl Bleed = 0mm, 3rd link = Middle)

Table. 3 Total pressure loss estimation (subsonic diffuser)

	Test Result	2 internal shocks	3 internal shocks	design
Throat Mach Number		2.61	2.13	1.57
Throat Pressure Recovery		0.808	0.778	0.711
Terminal Shock Mach Number		0.50	0.56	0.70
Terminal Shock Pressure Recovery		0.368	0.515	0.654
Interaction Loss		0.08	0.08	0.07
Separation Loss		0.01	0.01	0.02
Expected Pressure Recovery	0.15	0.28	0.43	0.56

(Ramp Bleed 20mm, Cowl Bleed - 0mm, 3rd link - Middle)

Table. 4 Mass flow estimation

		Flow Ratio
Design	1st ramp spillage	0.062
	2nd ramp spillage	0.010
	sideway spillage	0.014
	Flow Rate through Cowl Inlet	0.914
Test Result	Intake Mass Flow Ratio	0.795
	Ramp Bleed Flow Ratio	0.023
	Cowl Bleed Fow Ratio	0.000
	Flow Rate through Cowl Inlet	0.772

(Ramp Bleed = 20mm, Cowl Bleed = 0mm, 3rd link = Middle)

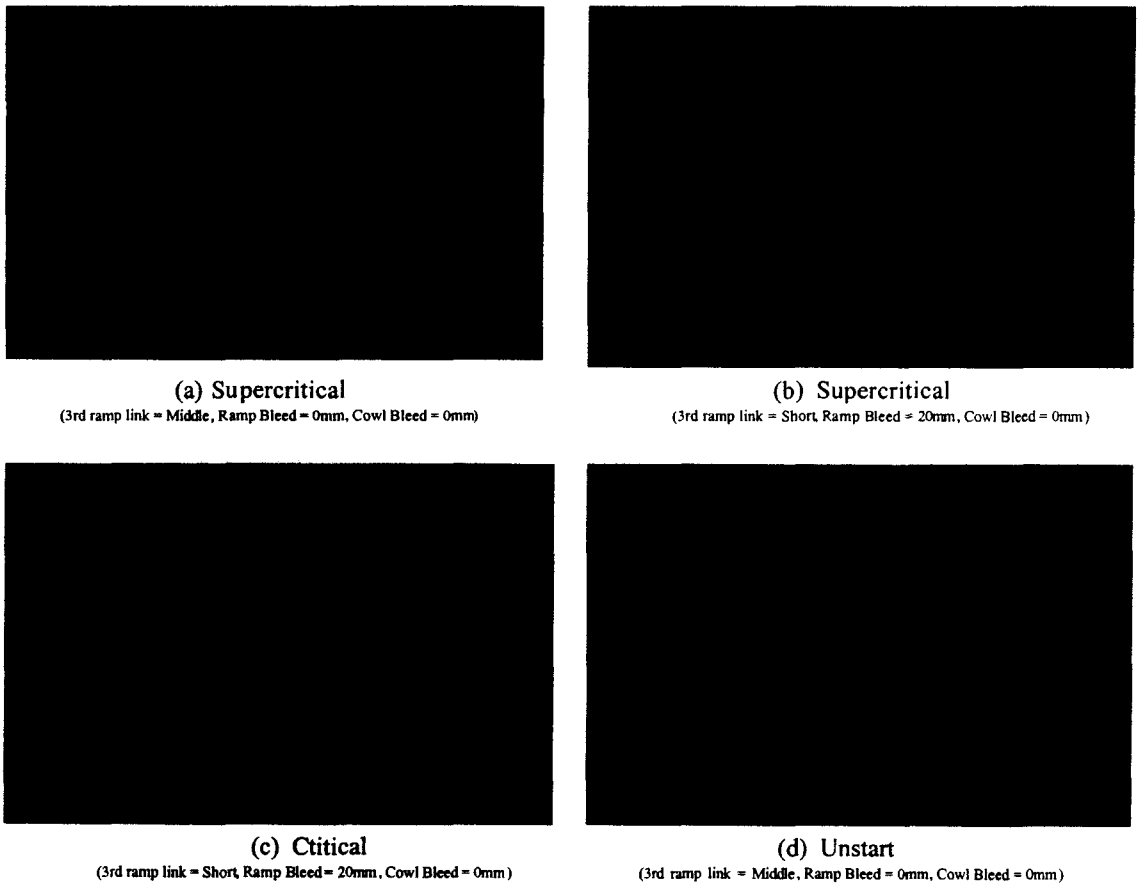

(a) Supercritical
(3rd ramp link = Middle, Ramp Bleed = 0mm, Cowl Bleed = 0mm)

(b) Supercritical
(3rd ramp link = Short, Ramp Bleed = 20mm, Cowl Bleed = 0mm)

(c) Ctitical
(3rd ramp link = Short, Ramp Bleed = 20mm, Cowl Bleed = 0mm)

(d) Unstart
(3rd ramp link = Middle, Ramp Bleed = 0mm, Cowl Bleed = 0mm)

Fig. 12 Schlieren Picture

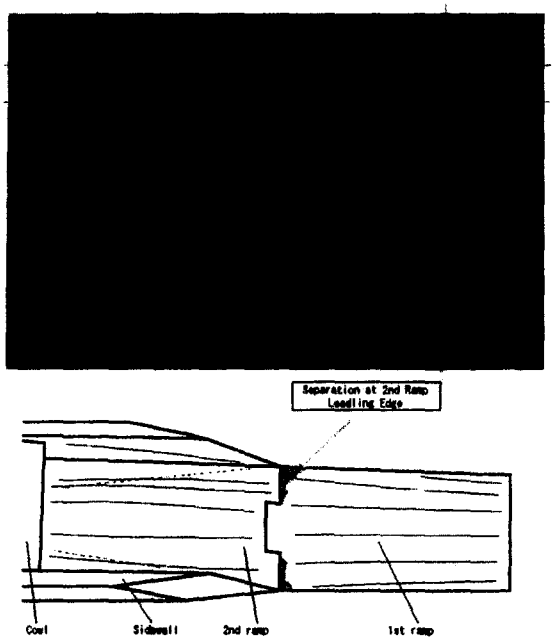

(a) View from cowl side

3rd ramp link = Short, Ramp Bleed = 20mm, Cowl Bleed = 0mm

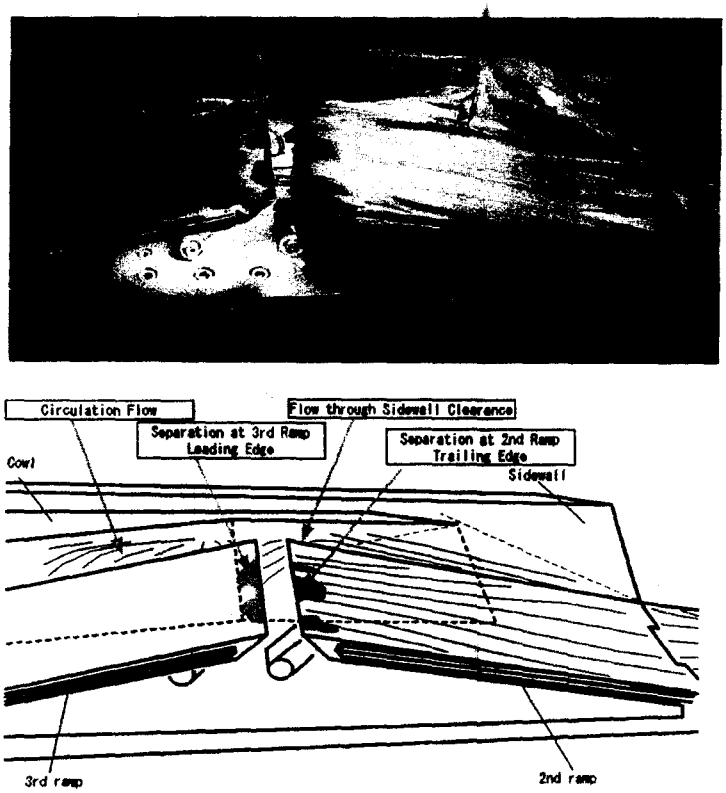

(a) View from sidewall side

3rd ramp link = Short, Ramp Bleed = 20mm, Cowl Bleed = 0mm

Fig. 13 Oilflow image